The type IV pilin PilA couples surface attachment and cell-cycle initiation in *Caulobacter crescentus*

Luca Del Medico[a], Dario Cerletti[a], Philipp Schächle[a], Matthias Christen[a,1], and Beat Christen[a,1]

[a]Institute of Molecular Systems Biology, Department of Biology, Eidgenössische Technische Hochschule Zürich, Zürich 8093, Switzerland

Edited by Christine Jacobs-Wagner, Yale University, New Haven, CT, and approved March 13, 2020 (received for review November 18, 2019)

Understanding how bacteria colonize surfaces and regulate cell-cycle progression in response to cellular adhesion is of fundamental importance. Here, we use transposon sequencing in conjunction with fluorescence resonance energy transfer (FRET) microscopy to uncover the molecular mechanism for how surface sensing drives cell-cycle initiation in *Caulobacter crescentus*. We identify the type IV pilin protein PilA as the primary signaling input that couples surface contact to cell-cycle initiation via the second messenger cyclic di-GMP (c-di-GMP). Upon retraction of pili filaments, the monomeric pilin reservoir in the inner membrane is sensed by the 17-amino acid transmembrane helix of PilA to activate the PleC-PleD two-component signaling system, increase cellular c-di-GMP levels, and signal the onset of the cell cycle. We termed the PilA signaling sequence CIP for "cell-cycle initiating pilin" peptide. Addition of the chemically synthesized CIP peptide initiates cell-cycle progression and simultaneously inhibits surface attachment. The broad conservation of the type IV pili and their importance in pathogens for host colonization suggests that CIP peptide mimetics offer strategies to inhibit surface sensing, prevent biofilm formation and control persistent infections.

Caulobacter crescentus | c-di-GMP | type IV pilin | TnSeq | FRET microscopy

The cell-cycle model bacterium *Caulobacter crescentus* (*Caulobacter* hereafter) integrates surface colonization into a biphasic life cycle. Attachment begins with a reversible phase, mediated by surface structures such as pili and flagella, followed by a transition to irreversible attachment mediated by polysaccharides (1–4). In *Caulobacter*, surface sensing is intimately interlinking with cellular differentiation and cell-cycle progression (5, 6). During the biphasic life cycle, *Caulobacter* divides asymmetrically and produces two distinct cell types with specialized development programs (Fig. 1*A*). The sessile stalked cell immediately initiates a new round of chromosome replication, whereas the motile swarmer cell, equipped with a polar flagellum and polar pili, remains in the G_1 phase for a defined interval before differentiating into a stalked cell and entering into the replicative S phase driven by the second messenger cyclic di-GMP (c-di-GMP)–dependent degradation of the cell-cycle master regulator CtrA (7, 8) (Fig. 1*A*). The change in cell-cycle state from motile swarmer into surface-attached replication-competent stalked cells depends on tactile sensing mechanisms. Both pili and flagella have been previously implicated as key determinants involved in tactile surface sensing (9–11). However, understanding the molecular mechanism of how *Caulobacter* interlinks bacterial surface attachment to cell-cycle initiation has remained elusive.

In this work, we report on a short peptide signal encoded within the type IVc pilin protein PilA that exerts pleiotropic control and links bacterial surface attachment to cell-cycle initiation in *Caulobacter*. Using fluorescence resonance energy transfer (FRET) microscopy in conjunction with a genetically encoded c-di-GMP biosensor (12), we quantify c-di-GMP signaling dynamics inside single cells and find that, besides its structural role in forming type IVc pili filaments, monomeric PilA in the inner membrane functions as a specific input signal that triggers c-di-GMP signaling at the G_1–S phase transition.

Results

A Specific Cell-Cycle Checkpoint Delays Cell-Cycle Initiation. To understand how bacterial cells adjust the cell cycle to reduced growth conditions, we profiled the replication time of the α-proteobacterial cell-cycle model organism *Caulobacter* across the temperature range encountered in its natural freshwater habitat (*SI Appendix*, Table S1). Under the standard laboratory growth temperature of 30 °C, *Caulobacter* replicates every 84 ± 1.2 min. However, when restricting the growth temperature to 10°C, we observed a 13-fold increase in the duration of the cell cycle, extending the replication time to 1,092 ± 14.4 min (*SI Appendix*, Table S1). To investigate whether reduced growth resulted in a uniform slowdown or affects particular cell-cycle phases, we determined the relative length of the G_1 phase by fluorescence microscopy using a previously described cell-cycle reporter strain (13) (*SI Appendix*). We found that the culturing of *Caulobacter* at 10°C caused a more than 1.4-fold increase in the relative duration of the G_1 phase, indicating a delay in cell-cycle initiation (Fig. 1*B*). This finding suggests the presence of a specific cell-cycle checkpoint that delays cell-cycle initiation during reduced growth conditions.

Significance

Pili are dynamic, long proteinaceous appendages found on the surface of many bacteria to promote adhesion. Here, we provide systems-level findings on a molecular signal transduction pathway that interlinks surface sensing with cell-cycle initiation. We propose that surface attachment induces depolymerization of pili filaments. The concomitant increase in pilin subunits within the inner membrane function as a stimulus to activate the second messenger cyclic di-GMP and trigger cell-cycle initiation. Furthermore, we show that the provision of a 17-amino acid synthetic peptide corresponding to the membrane portion of the pilin subunit mimics surface sensing, activates cell-cycle initiation, and inhibits surface attachment. Thus, synthetic peptide mimetics of pilin represent promising chemotypes to control biofilm formation and treat bacterial infections.

Author contributions: L.D.M., M.C., and B.C. designed research; L.D.M., D.C., and P.S. performed research; L.D.M., D.C., P.S., M.C., and B.C. analyzed data; and M.C. and B.C. wrote the paper with input from all authors.

The authors declare no competing interest.

This article is a PNAS Direct Submission.

[1]To whom correspondence may be addressed. Email: beat.christen@imsb.biol.ethz.ch or matthias.christen@imsb.biol.ethz.ch.

This article contains supporting information online at https://www.pnas.org/lookup/suppl/doi:10.1073/pnas.1920143117/-/DCSupplemental.

First published April 15, 2020.

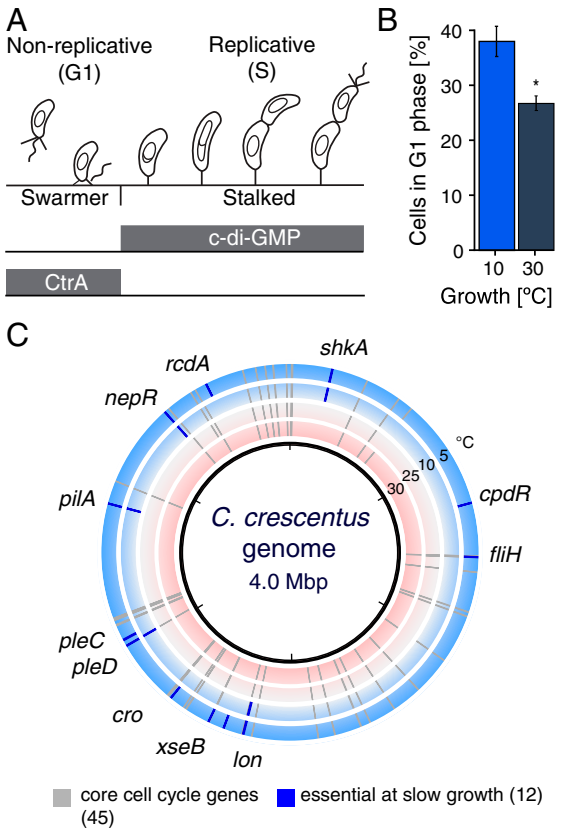

Fig. 1. TnSeq identifies conditionally essential genes required during reduced growth conditions. (*A*) *Caulobacter* divides asymmetrically into a replication-competent stalked cell and a swarmer cell. The master regulator CtrA inhibits DNA replication in swarmer cells and is proteolytically cleared upon an increase in cellular levels of the second messenger c-di-GMP at the G_1–S phase transition. (*B*) Cellular replication under slow-growth conditions increases the relative duration of the G_1 phase as determined by a fluorescently tagged cell-cycle reporter strain. (*C*) TnSeq across the 4.0-Mbp *Caulobacter* genome defines 45 core-essential cell-cycle genes (gray marks) to sustain growth at 5°C, 10°C, 25°C, and 30°C (outer to inner track) and 12 conditionally essential genes required for slow-growth conditions (blue marks). (*D*) Hierarchical clustering analysis of the 12 conditionally essential genes required during reduced growth conditions.

TnSeq Identifies Conditionally Essential Cell-Cycle Genes. To identify the complete set of genes required for cell-cycle progression at different growth rates, we designed a systems-wide forward genetic screen based on quantitative selection analysis coupled to transposon sequencing (TnSeq) (14, 15). TnSeq measures genome-wide changes in transposon insertion abundance upon subjecting large mutant populations to different selection regimes and enables genome-wide identification of essential genes. We hypothesized that the profiling of growth rate-dependent changes in gene essentiality will elucidate the components of the cell-cycle machinery fundamental for cell-cycle initiation under reduced growth conditions. We selected *Caulobacter* transposon mutant libraries for prolonged growth at low temperatures (5°C and 10°C) and under standard laboratory cultivation conditions (25°C and 30 °C). Cumulatively, we mapped, for each condition, between 397,377 and 502,774 unique transposon insertion sites across the 4.0-million base pairs (Mbp) *Caulobacter* genome corresponding to a transposon insertion density of 4 to 5 bp (*SI Appendix*, Table S2).

To identify the factors required for cell-cycle progression, we focused our analysis on essential genes (Dataset S1) that are expressed in a cell-cycle–dependent manner (*SI Appendix* and refs. 16–18). Among 373 cell-cycle–controlled genes, we found 45 genes that were essential under all growth conditions (Fig. 1*C* and Dataset S1), including five master regulators (*ctrA*, *gcrA*, *sciP*, *ccrM*, and *dnaA*), 11 divisome and cell wall components (*ftsABILQYZ*, *fzlA*, and *murDEF*), and six DNA replication and segregation factors (*dnaB*, *ssb*, *gyrA*, *mipZ*, *parB*, and *ftsK*), as well as 23 additional genes encoding key signaling factors and cellular components required for cell-cycle progression (Dataset S1). Collectively, these 45 genes form the core components of the bacterial cell-cycle machinery.

Components of the c-di-GMP Signaling Network Are Conditionally Essential for Slow Growth. During reduced growth conditions, we found 12 genes that specifically became essential (Fig. 1*C*). To gain insights into the underlying genetic modules, we performed a hierarchical clustering analysis and grouped these 12 genes according to their growth rate-dependent fitness profile into three functional clusters, A, B, and C (Fig. 1*D* and *SI Appendix*).

Cluster A contained four conditionally essential genes that exhibited a large decrease in fitness during slow-growth conditions (Fig. 1*D* and *SI Appendix*, Fig. S1). Among them were *pleD*, *cpdR*, *rcdA*, and *lon* that all comprise important regulators for cell-cycle–controlled proteolysis. The diguanylate cyclase PleD produces the bacterial second messenger c-di-GMP, which becomes restricted to the stalked cell progeny upon asymmetric cell division and is absent in the newly born swarmer cell (Fig. 1*A* and ref. 12). During the G_1–S phase transition, c-di-GMP levels rise again and trigger the proteolytic clearance of the cell-cycle master regulator CtrA (Fig. 1*A*), which is mediated by ClpXP and the proteolytic adaptor proteins RcdA, CpdR, and PopA (19–22). Similarly, the ATP-dependent endopeptidase Lon is responsible for the degradation of the cell-cycle master regulators CcrM, DnaA, and SciP (23–25). Taken together, these findings underscore the importance of controlling proteolysis of CtrA and other cell-cycle regulators to maintain cell-cycle progression at low growth rates when intrinsic protein turnover rates are marginal (26).

Cluster B contained five genes, including the two histidine kinase genes *pleC* and *shkA*, a gene of unknown function encoding a conserved hypothetical protein (CCNA_02103), and the type IV pilin gene *pilA* and the flagellar assembly ATPase *flbE*/*fliH* (Fig. 1*D* and *SI Appendix*, Fig. S2). Multiple genes of cluster B participate in c-di-GMP signaling. Among them, we found the sensor kinase PleC that functions upstream and activates the diguanylate cyclase PleD over phosphorylation. The hybrid kinase ShkA comprises a downstream effector protein of PleD, which binds c-di-GMP and phosphorylates the TacA transcription factor responsible for the initiation of the stalked cell-specific transcription program (27, 28). The flagellum assembly

ATPase FlbE/FliH together with FliI and FliJ form the soluble component of the flagellar export apparatus, which, in *Pseudomonas*, has also been identified as a c-di-GMP effector complex (29). Collectively, these data indicate that c-di-GMP signaling is of fundamental importance to coordinate cell-cycle progression under slow-growth conditions.

Cluster C comprised the antisigma factor *nepR*, a Cro/CI transcription factor (CCNA_02315), and *xseB* encoding the small subunit of the exodeoxyribonuclease VII (Fig. 1*D* and *SI Appendix*, Fig. S3), which form outer-circle components not directly linked to c-di-GMP signaling. However, disruption of these genes likely induces stress responses and alternative transcriptional programs that may interfere with cell-cycle progression under slow-growth conditions.

PilA Induces c-di-GMP Signaling to Initiate Cell-Cycle Progression. Among the components of the c-di-GMP signaling network identified within clusters A and B, the sensor kinase PleC resides at the top of the signaling hierarchy activating the diguanylate cyclase PleD at the G_1–S phase transition. While the activation mechanism of its downstream target PleD has been resolved in molecular detail (30), the type of external signal integrated by PleC has remained unknown. PleC comprises an amino-terminal periplasmic domain, which suggests that PleC activity is controlled by an external signal. Among the identified conditionally essential genes within cluster B, PilA coclustered together with PleC (Fig. 1*D*). The C-terminal portion of the type IV pilin protein PilA is translocated into the periplasm. Furthermore, PilA shares the same subcellular localization pattern to the swarmer-specific cell pole as PleC (13, 31). Thus, we speculated that PilA is a likely candidate for the hitherto unknown external input signal perceived by the sensor kinase PleC.

To test this hypothesis, we monitored the c-di-GMP signaling dynamics in a wild-type and Δ*pilA* background. The activation of PleC, and subsequently PleD, leads to a strong increase in the c-di-GMP levels at the G_1–S phase transition (Fig. 1*A* and ref. 12). Any mutation that impairs activation of the PleC kinase function is expected to prolong the G_1 swarmer phase. To monitor c-di-GMP signaling dynamics inside single cells, we have previously engineered a genetically encoded FRET biosensor that permits time-resolved monitoring of the fluctuating c-di-GMP levels along the cell cycle (12). We synchronized wild-type and Δ*pilA* cells expressing this FRET biosensor and quantified c-di-GMP levels in individual swarmer cells by FRET microscopy (Fig. 2*A* and *SI Appendix*). In the wild-type control, we observed that the majority of synchronized cells quickly transitioned into the S phase, with only 11.8% (143 out of 1,216 cells) remaining in the G_1 phase, as indicated by low c-di-GMP levels (Fig. 2 *A* and

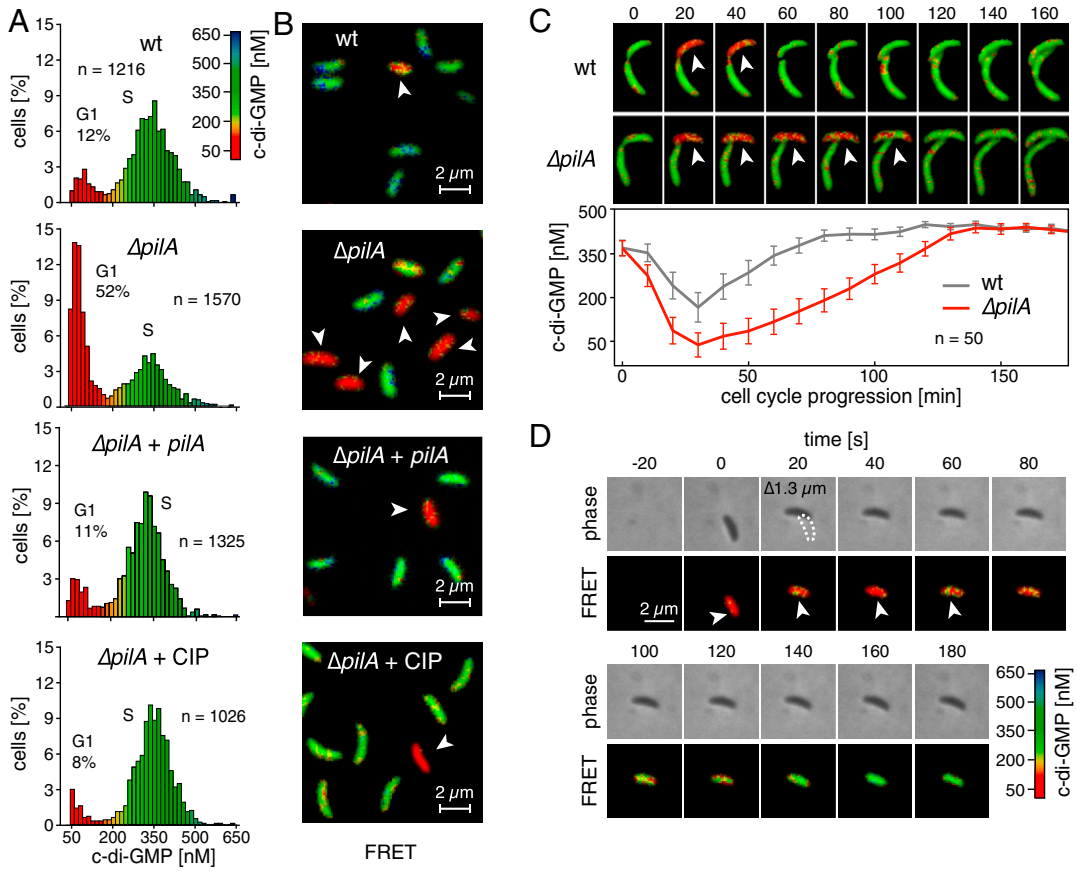

Fig. 2. The type IV pilin PilA functions as cell-cycle initiating signal. (*A*) Population distribution of intracellular c-di-GMP concentrations in synchronized *Caulobacter* cells. The population shows a bimodal c-di-GMP distribution corresponding to swarmer cells (G_1) and cells that underwent G_1 to S transition (S). (*B*) Dual-emission ratio microscopic (FRET) images of synchronized swarmer populations of wild-type *Caulobacter*, Δ*pilA* mutants, Δ*pilA* complemented by a plasmid-born copy of *pilA*, and Δ*pilA* complemented by the exogenous addition of the CIP peptide (100 μM). Pseudocolors show FRET emission ratios (527/480 nm) corresponding to the cytoplasmic c-di-GMP concentration as indicated by the color bar. Swarmer cells (highlighted by arrows) resting in the G_1 phase prior initiation of cell cycle exhibit low cellular c-di-GMP levels. (*C*) (*Top*) Time-lapse FRET microscopy following cell-cycle progression and (*Bottom*) corresponding plots of the quantified c-di-GMP levels over a population of 50 swarmer cells are shown for wild type (gray) and Δ*pilA* (red) at 10-min intervals. Scale similar to *D*. (*D*) Time-lapse FRET microscopy and phase-contrast images of a *Caulobacter* swarmer cell (white arrows) attaching to an agar surface. The cell attaches at time point 0 s and pulls itself over a distance of 1.3 μm (white contour) prior increasing the cellular c-di-GMP level.

B). In contrast, we observed that more than 52.2% (821 out of 1,570 cells) of all of the synchronized Δ*pilA* mutant cells exhibited a delay in the G_1–S transition and maintained low c-di-GMP levels for a prolonged interval (Fig. 2 *A* and *B*). Consistent with an increase in the duration of the G_1 phase, we also observed that Δ*pilA* swarmer cells exhibited a 7.7% increase in cell length compared to wild-type swarmer cells (*SI Appendix*, Table S3). Similarly, using time-lapse studies to follow signaling trajectories of individual cells, we found that Δ*pilA* mutants exhibited a more than 1.7-fold increase in the duration of the G_1 phase as compared to wild-type cells (65 ± 3 min versus 38 ± 1 min for Δ*pilA* and wild type, respectively; Fig. 2*C* and *SI Appendix*, Table S4). Providing an episomal copy of *pilA* restored the cell-cycle timing defect of a Δ*pilA* mutant strain (Fig. 2 *A* and *B*). When following the formation of duplicated replication origins in synchronized cells using a fluorescent CFP-ParB reporter (32, 33), we observed that a Δ*pilA* mutant showed a 1.4-fold lower proportion of cells that entered S phase as compared to wild type (18.9 ± 1.2% versus 26.5 ± 1.2% at 37 min after synchrony; *SI Appendix*, Fig. S4*B* and Table S5). Furthermore, when monitoring c-di-GMP signaling dynamics in attaching swarmer cells through time-lapse FRET microscopy, we observed that, upon surface contact, swarmer cells showed, within seconds, a cell body displacement, consistent with pili retraction in the micrometer range, which preceded a rapid rise in cellular c-di-GMP levels (Fig. 2*D* and Movie S1). Collectively, these findings establish the type IV pilin PilA as an input signal interlinking surface attachment with cell-cycle progression and initiation of chromosome replication.

PilA Controls Cell-Cycle Initiation via the Sensor Kinase PleC and the Diguanylate Cyclase PleD. PleC is a bifunctional phosphatase/kinase that switches activity in a cell-cycle–dependent manner (34). In the newborn swarmer cell, PleC first assumes phosphatase activity to inactivate the diguanylate cyclase PleD and establish low cellular c-di-GMP levels. Subsequently, PleC switches to a kinase and activates PleD at the G_1–S phase transition. To test whether PilA functions as an input signal for the PleC-PleD signaling cascade, we measured c-di-GMP signaling dynamics and compared the duration of the G_1 phase in single- and double-deletion mutants using FRET microscopy (*SI Appendix*, Fig. S5). Similar to Δ*pilA* mutants, Δ*pleD* mutants also prolonged the G_1 phase more than twofold as compared to the wild-type control (18% and 22% versus 9% G_1 cells in wild type; *SI Appendix*, Fig. S5). However, a Δ*pilA*, Δ*pleD* double mutant only marginally increased the duration of the G_1 phase and showed similar frequencies of swarmer cells with low-c-di-GMP levels as compared to a strain lacking solely *pleD* (28% and 22% G_1 cells; *SI Appendix*, Fig. S5). This genetic evidence suggests that PilA resides upstream of PleD. Thus, besides its role as a structural component of the type IVc pilus, PilA likely comprises an input signal for the sensor kinase PleC, which serves as the cognate kinase of PleD, to increase c-di-GMP levels at the G_1–S phase transition.

The Inner Membrane Reservoir of the Type IV Pilin PilA Signals Cell-Cycle Initiation. PilA harbors a short 14-amino acid N-terminal leader sequence required for the translocation across the inner membrane that is cleaved off by the peptidase CpaA (35–37). To test whether the translocation of PilA is a prerequisite for signaling the cell-cycle initiation, we constructed a cytosolic version of PilA ($pilA_{15–59}$) lacking the N-terminal leader sequence needed for the translocation of the matured PilA across the membrane. Unlike the full-length PilA, the episomal expression of the translocation-deficient version of PilA did not complement the cell-cycle timing defect of a Δ*pilA* mutant (Fig. 3*A* and *SI Appendix*, Fig. S6 and Table S6). Similarly, we found that solely expressing the N-terminal leader sequence of PilA ($pilA_{1–14}$) did not restore the cell-cycle timing defects of a Δ*pilA* mutant (Fig. 3*A* and *SI Appendix*, Fig. S6 and Table S6). We concluded that the translocation of PilA into the periplasm is a prerequisite to signal cell-cycle initiation.

Upon translocation and cleavage of the N-terminal leader sequence, the mature form of PilA resides as a monomeric protein anchored in the inner membrane (38). Through the action of a dedicated type IV pilus assembly machinery, the inner membrane-bound reservoir of PilA polymerizes into polar pili filaments that mediate initial attachment to surfaces (39). However, only *pilA*, but none of the other components of the pilus assembly machinery, became essential in our TnSeq screen under slow-growth conditions (Fig. 1*C*, *SI Appendix*, Table S7, and Dataset S1). Furthermore, unlike Δ*pilA* mutants, deletion mutants of the pilus assembly machinery genes *cpaA*, *cpaD*, and *cpaE* did not prolong the G_1 phase but, in contrast, shortened the duration of the G_1 phase by twofold as compared to the wild-type control (4%, 3%, and 5% G_1 cells; *SI Appendix*, Fig. S5). The observation that the translocation of PilA monomers across the inner membrane is necessary but that the subsequent polymerization of PilA monomers into pilin filaments is dispensable for cell-cycle initiation suggested that the inner membrane reservoir of the monomeric form of PilA functions as an input signal for c-di-GMP–mediated cell-cycle signaling.

The Transmembrane Helix of PilA Comprises a 17-Amino Acid Peptide Signal That Mediates Cell-Cycle Initiation. The mature form of PilA is a small 45-amino acid protein comprising a highly hydrophobic N-terminal alpha helix, which anchors PilA in the inner membrane (36, 38), and an adjacent variable alpha-helical domain protruding into the periplasm. To identify the portion of the matured PilA protein responsible for triggering cell-cycle initiation, we constructed a panel of C-terminally truncated *pilA* variants and assessed their ability to complement the cell-cycle defect of a chromosomal Δ*pilA* mutant by quantifying c-di-GMP dynamics in single cells using FRET microscopy (*SI Appendix*). The expression of a truncated PilA variant that includes the leader sequence and the first five N-terminal amino acids of the matured PilA protein (PilA 5aa) did not complement the cell-cycle initiation defect of a Δ*pilA* mutant (Fig. 3*A* and *SI Appendix*, Fig. S6 and Table S6). However, increasing the N-terminal portion of the matured PilA protein to 17, 25, and 37 amino acids (PilA 17aa, PilA 25aa, and PilA 37aa) restored the cell-cycle initiation defects of a Δ*pilA* mutant (Fig. 3*A* and *SI Appendix*, Fig. S6 and Table S6). Based on these findings, we concluded that a small N-terminal peptide sequence covering only 17 amino acids from the mature PilA (Fig. 3*A*) is sufficient to initiate c-di-GMP–dependent cell-cycle progression. Accordingly, we annotated this peptide sequence as cell-cycle initiating pilin (CIP) sequence (Fig. 3*A*).

Chemically Synthesized CIP Peptide Initiates Cell-Cycle Progression. Next, we asked whether the translocation of PilA from the cytoplasm or the presence of a PilA reservoir in the periplasm is sensed. If signaling depends solely on the presence of membrane-inserted PilA, we speculated that exogenous provision of chemical-synthesized CIP peptide should restore the cell-cycle defects in a Δ*pilA* mutant. To test this hypothesis, we incubated synchronized swarmer cells of a Δ*pilA* mutant in the presence of 100 μM of chemically synthesized CIP peptide and assayed c-di-GMP signaling dynamics by FRET microscopy (Fig. 2 *A* and *B*). Indeed, we found that addition of the CIP peptide induced cell-cycle transition into the S phase as indicated by a more than twofold lower abundance of G_1 swarmer cells with low c-di-GMP levels as compared to an untreated Δ*pilA* cell population (8% vs. 17% G_1 cells, upon 15 min incubation of synchronized swarmer cells with CIP or the mock control, Fig. 2 *A* and *B*). These findings suggest that the addition of

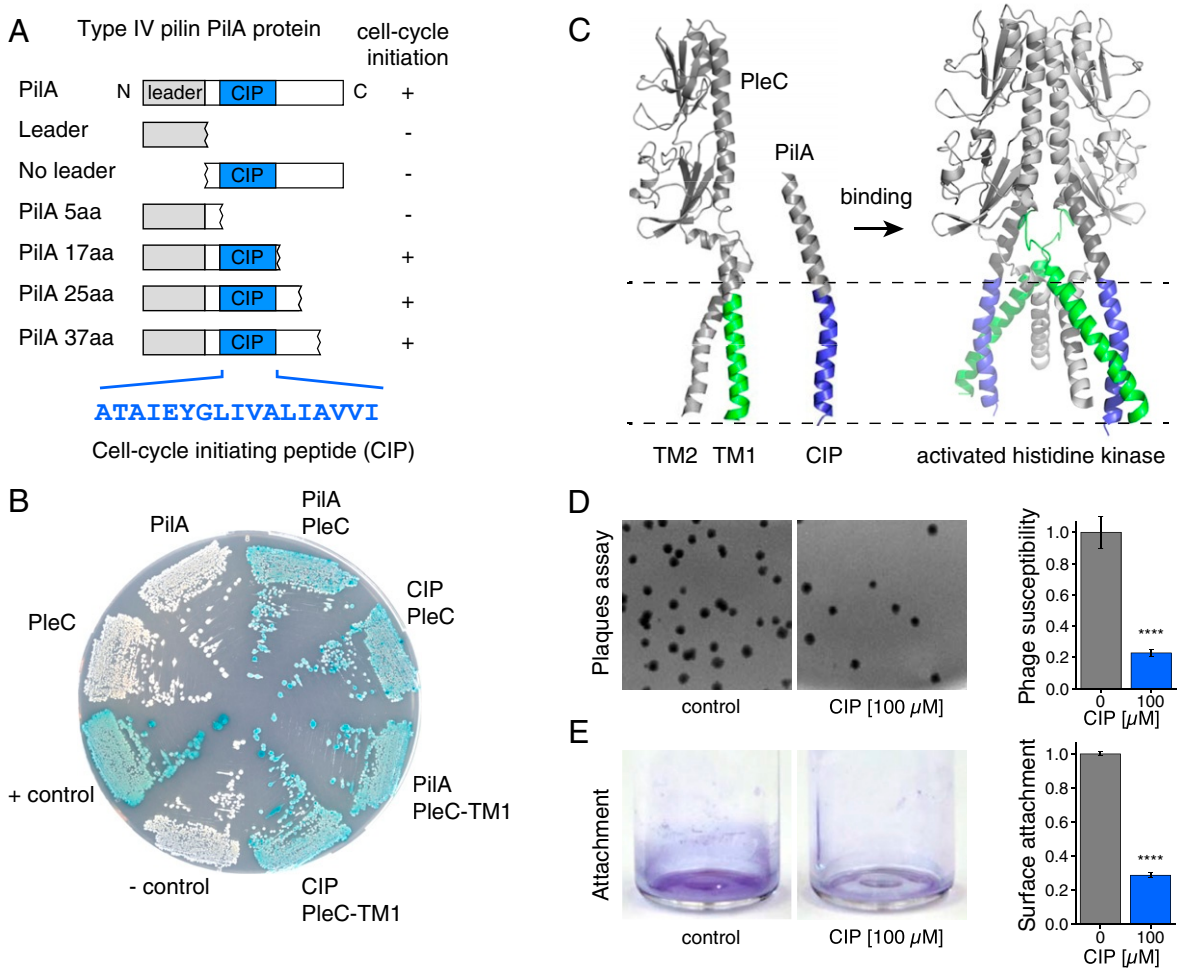

Fig. 3. Genetic mapping, pleiotropic effects, and proposed mode of action of the CIP peptide. (*A*) Complementation of the cell-cycle initiation defect of Δ*pilA* with a panel of N- and C-terminal truncated PilA variants. (*B*) The periplasmic sensor domain of PleC (PleC2-315) or a fragment covering only the first transmembrane helix (TM1, PleC2-50) interact with the matured PilA (PilA2-59) or the CIP peptide portion of PilA (CIP, PilA2-31) as detected by the BACTH (40) using X-Gal reporter plates. Cleavage-deficient PilA variants (PilAΔDE11,12) were used to prevent processing of T18-PilA fusion in *E. coli*. (*C*) (*Left*) Structural homology modeling of the periplasmic domain of PleC with the SWISS-MODEL server (41) suggests similarity with the family of chemoreceptor domains (42) that possess two transmembrane helices (TM1, TM2). Dashed lines highlight the membrane region. The *Caulobacter* pilin PilA was modeled onto the type IV pilin from *Neisseria* (1AY2). The TM1 (green) interacts with the CIP peptide portion of PilA (blue). (*Right*) Binding of PilA (in blue) to the the TM1 portion (green) of the PleC sensor domain will induce structural rearrangement between the dimerized four helical bundles in the transmembrane region to induce autophosphorylation at the conserved histidine residues in the cytoplasmic kinase domain. (*D*) ΦCbk phage susceptibility assay and corresponding bar chart of *Caulobacter* CB15 in the (*Right*) presence and (*Left*) absence of 100-μM chemically synthesized CIP peptide ($n = 5$). (*E*) Crystal violet staining and corresponding bar chart of the relative surface attachment of *Caulobacter* CB15 upon 1 h of incubation without ($n = 9$) or with ($n = 9$) 100-μM CIP peptide. Error bars are SEM; $^{****}P << 10^{-4}$.

the CIP peptide shortens the G_1 phase and, thus, functions as a cell-cycle activator. Collectively, these results demonstrated that neither the translocation nor polymerization but solely the inner membrane reservoir of PilA is sensed via the hydrophobic CIP sequence to initiate cell-cycle progression.

The Periplasmic Domain of PleC Senses the CIP Peptide. Deletion of the sensor kinase *pleC* causes daughter cells to omit the G_1 phase with low c-di-GMP levels (*SI Appendix*, Fig. S5 and ref. 12). The observation that the addition of the CIP peptide shortens the G_1-phase suggests that the CIP sequence of PilA modulates PleC activity to promote phosphorylation of the downstream effector PleD. To test whether PilA directly interacts with the periplasmic domain of PleC, we used a bacterial two-hybrid assay (BACTH) and measured protein–protein interactions in *Escherichia coli* through reconstitution of the adenylate cyclase from the T18 and T25 split domains (40). T18-domain fusions of PilA (T18-PilA2-59) or only the CIP sequence (T18-PilA2-31) interacted with T25-domain fusions of the intact periplasmic domain of PleC (T25-PleC2-315) (Fig. 3*B* and *SI Appendix*, Table S8). The periplasmic PleC domain comprises two transmembrane helices (TM1 and TM2, positioned at residues 28 to 50 and 283 to 305). To further characterize the binding site of the CIP peptide, we assayed truncated variants of the periplasmic PleC domain. We found that an N-terminal PleC fragment covering solely the TM1 (T25-PleC2-50) was sufficient for interaction with PilA (T18-PilA2-59) or the CIP peptide (T18-PilA2-31) (Fig. 3*B* and *SI Appendix*, Table S8).

Structural homology modeling (SWISS-MODEL) (41) revealed that the periplasmic domain of PleC exhibits predicted structural similarity with the family of dimeric chemoreceptor domains [Fig. 3*C*; Mlp37 from *V. cholera* (42, 43)]. These receptor domains harbor two TM helices that transmit ligand-induced signaling across the membrane to regulate the activity of cytoplasmic kinase and other output domains (44). In agreement with a binding mode involving membrane helix

interactions, the PilA structural model consists of a single transmembrane-spanning alpha helix (Fig. 3*C*). How could binding of the CIP peptide to TM1 of the periplasmic domain of PleC lead to activation of the output kinase domain? One possibility is that binding of the CIP peptide to the PleC receptor domain induces a structural rearrangement between the dimerized four helical bundles in the transmembrane region to activate autophosphorylation of the cytoplasmic kinase domain (Fig. 3*C*). In support of a ligand-induced conformational rearrangement in the receptor complex, we observed that T18 and T25 fusions to the N-terminal portion of PleC spanning the TM1, the periplasmic domain, and the TM2 (T18-PleC2-315 and T25-PleC2-315) showed strong interaction, but detected a more than 39% reduction in adenylate cyclase activity when coexpressing also the CIP peptide (*SI Appendix*, Table S9). Collectively, these findings suggest that the histidine kinase PleC senses the membrane-inserted PilA pool through direct interaction between the CIP sequence and the first transmembrane helix (TM1) of the periplasmic receptor domain.

The CIP Peptide Reduces Surface Attachment and ΦCbk Phage Susceptibility. In addition to omitting the G_1 phase, deletion of the sensor kinase *pleC* also results in pleiotropic defects including a lack of polar pili and defects in initial attachment to surfaces (45). To gain further evidence that PilA, upon binding, modulates the activity of the sensor kinase PleC, we investigated whether the addition of the chemically synthesized CIP peptide also impairs additional PleC-specific output functions. Indeed, when assaying for the presence of functional pili using the pili-specific bacteriophage ΦCbK, we found that incubating synchronized wild-type *Caulobacter* for 10 min with the CIP peptide resulted in a 77.2 ± 2.1% decrease in bacteriophage CbK susceptibility (Fig. 3*D*), suggesting that binding of the CIP peptide impairs pili function. Furthermore, we also found that the addition of the CIP peptide to wild-type *Caulobacter* CB15 cells reduced initial attachment by 71.3 ± 1.6% (Fig. 3*E*), with a half-effective peptide concentration (EC_{50}) of 8.9 μM (*SI Appendix*, Fig. S7) and a Hill coefficient of 1.6, suggesting positive cooperativity in the binding of CIP to a multimeric PleC receptor complex. Altogether, these findings support a model in which the CIP sequence of PilA functions as a pleiotropic small-peptide modulator of the sensor kinase PleC, leading to premature cell-cycle initiation, retraction of type IV pili, and impairment of surfaces attachment.

Discussion

Understanding how bacteria regulate cell-cycle progression in response to external signaling cues is of fundamental importance. In this study, we used a TnSeq approach to identify genes required for cell-cycle initiation. Comparing deviations in gene essentiality between growth at low temperatures (5°C and 10°C) and under standard laboratory cultivation conditions (25°C and 30 °C) allowed us to pinpoint genes required exclusively for cell-cycle initiation. We identified the pilin protein PilA together with six additional components of a multilayered c-di-GMP signaling network (Fig. 1) as key determinants that control cell-cycle initiation. Using FRET microscopy studies, we quantified c-di-GMP signaling dynamics inside single cells and found that, besides its structural role in forming type IVc pili filaments, PilA comprises a specific input signal for activation of c-di-GMP signaling at the G_1–S phase transition (Fig. 4). Furthermore, we show genetic evidence that PilA functions upstream of the PleC-PleD two-component signaling system and present data that the monomeric PilA reservoir is sensed through a short 17-amino-acid-long N-terminal peptide sequence (CIP), which directly interacts with the first transmembrane helix anchoring the periplasmic domain of the sensor kinase PleC (Fig. 4). It is remarkable that the *Caulobacter* PilA is a multifunctional protein that encodes, within a 59-amino acid polypeptide, a leader sequence for translocation, the CIP sequence for cell-cycle signaling functions, and structural determinants required for pili polymerization.

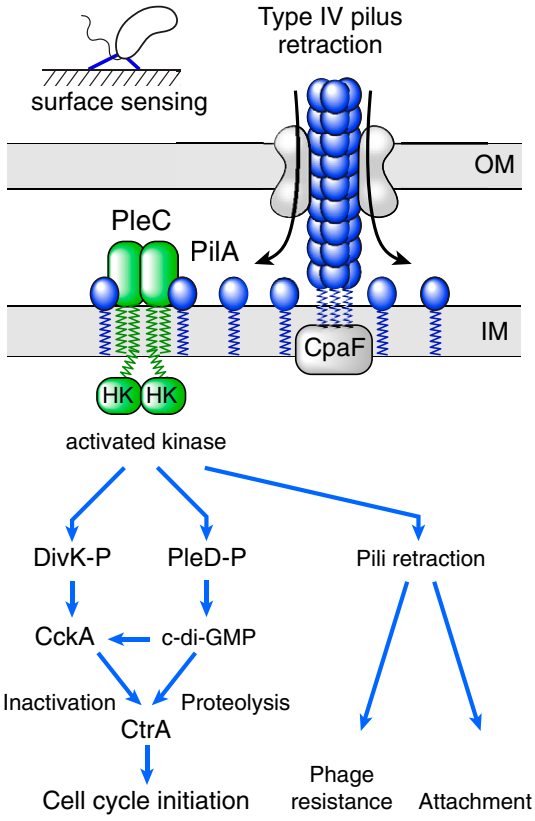

Fig. 4. Model of the type IV pilin-mediated signaling network coupling surface sensing with cell-cycle initiation. Surface-induced retraction of type IV pili leads to accumulation of monomeric PilA in the inner membrane, where PilA interacts with the transmembrane portion of the sensor kinase PleC. Binding of PilA activates the kinase function of PleC to promote phosphorylation of the downstream effectors PleD and DivK, and activates pili retraction as part of a positive feedback loop. DivK and PleD synergistically promote inactivation and degradation of the master regulator CtrA to initiate cell-cycle progression.

Caulobacter exhibits a biphasic life cycle where newborn swarmer progeny undergo an obligate differentiate into surface-attached stalked cells to initiate DNA replication. How could PilA couple cell-cycle initiation to surface sensing? Type IV pili have been shown to serve as adhesion filament as well as mechanosensors (38, 46, 47), that, upon surface contact, induce the retraction of pili filaments with concomitant accumulation of monomeric PilA in the inner membrane (9). Our results from genetic dissection of PilA in conjunction with FRET microscopy to monitor c-di-GMP signaling dynamics upon surface contact (Fig. 2*D* and Movie S1) suggest a model where high levels of PilA monomers in the inner membrane are sensed via the N-terminal CIP sequence that binds and activates the sensor kinase PleC to promote phosphorylation of the diguanylate cyclase PleD (Fig. 4). In such a model, surface sensing by pili induces a sharp increase in intracellular c-di-GMP levels and activates the proteolytic clearance (19, 21) of the master regulator CtrA to initiate cell-cycle progression (Fig. 4).

In support of this model, parallel studies conducted by the laboratory of Yves Brun and colleagues show that chemical or genetic obstruction of pili retraction leads to an increase in the cellular c-di-GMP pool, premature replication initiation, polar remodeling, and stalked-cell differentiation (48). However, the precise structural mechanism of how initial surface contact

stimulates pili retraction remains an open question. In *Caulobacter*, studies showed that pili, upon covalent attachment of high-molecular-weight conjugates, lose their dynamic activities (9). One possibility is that, upon surface contact, force generation leads to structural rearrangements within the filament that locks pili in the retraction state, which, in turn, prevents pilus extension and reincorporation of subunits, leading to elevated PilA levels in the inner membrane and subsequent activation of c-di-GMP signaling. Recent work showed that the second-messenger c-di-GMP itself also affects pilus dynamics, promoting increased activity at intermediate levels and retraction of pili at peak concentrations (49). Thus, blocking retraction of an individual pilus likely induces a positive feedback loop to induce retraction of additional pili at the cell pole, leading to robust surface sensing.

Using BACTHs, we find that PilA binds via the membrane-embedded CIP portion to the transmembrane bundle of the periplasmic receptor domain of the sensor kinase/phosphatese PleC (Fig. 3 *B* and *C* and *SI Appendix*, Tables S8 and S9). Binding of pilins to histidine kinases via transmembrane interactions has also been reported in *Pseudomonas aeruginosa*, where pilins regulate their own expression via direct intramembrane interactions with the sensor kinase PilS (50). In contrast to PleC, PilS possesses a different N-terminal sensor domain, and binding of PilA to PilS was reported to switch the kinase into the phosphatase state (50). Thus, convergent signaling mechanisms sensing the inner membrane pool of pilins have evolved in different organism to regulate distinct output functions, including surface-induced cell-cycle initiation and pili biogenesis.

On the level of signal integration, sensing the PilA reservoir through the bifunctional kinase/phosphatase PleC provides robust signal integration to sense surfaces. Small fluctuations in the inner membrane PilA concentrations due to dynamic pili cycling in the planktonic state do not lead to a permanent increase in cellular c-di-GMP levels, as PleC kinase activity induced upon retraction is reversed when pili are extended again and PleC is reset to a phosphatase. In a model where surface contact locks pili in the retraction state, the kinase activity of PleC wins the tug of war, leading to a permanent increase in c-di-GMP levels and a robust surface sensing mechanism.

From an engineering perspective, coupling surface sensing via the inner membrane PilA reservoir to a c-di-GMP second-messenger cascade provides a mechanism to couple cell-cycle initiation to multiple orthogonal output functions, including inhibition of flagellar motility (51), secretion of adhesive surface polysaccharides (9), and activation of stalk cell-specific transcriptional programs (28) to induce permanent surface attachment and cellular differentiation at the G_1–S phase transition.

The bacterial second-messenger cyclic diguanylate (c-di-GMP) is a key regulator of cellular motility, cell-cycle initiation, and biofilm formation with its resultant antibiotic tolerance, which can make chronic infections difficult to treat (52–54). In our work, we show that the addition of a chemically produced CIP peptide specifically modulates the c-di-GMP signaling behavior in cells (Fig. 2*A*) and also has pleiotropic effects on surface adhesion and phage susceptibility in *Caulobacter* (Fig. 3 *D* and *E*). Therefore, the CIP peptide, regulating the spatiotemporal production of c-di-GMP, might be an attractive drug target for the control of biofilm formation that is part of chronic infections. Whether the chemical-synthesized CIP peptide can penetrate the outer membrane on its own or is taken up via the CpaC secretion channel or other porins remains to be determined. Given the broad conservation of type IV pili and their central role in human pathogens to drive infection and host colonization (55), the CIP peptide identified represents a promising chemotype and is potentially developable into a chemical genetic tool to dissect c-di-GMP signaling networks and to block surface sensing in pathogens to treat bacterial infections.

Materials and Methods

SI Appendix includes detailed descriptions of strains, media and standard growth conditions, Tn*5* transposon mutagenesis, growth selection and sequencing, FRET microscopy procedures to quantify cellular c-di-GMP levels in *Caulobacter* cells, CIP peptide assay, quantification of surface attachment, and phage susceptibility assays. Dataset S1 contains the essentiality classification of each cell-cycle–controlled *Caulobacter* gene profiled at different growth temperatures according to TnSeq measurements.

TnSeq Library Generation. Tn*5* hypersaturated transposon mutant libraries in *Caulobacter* were generated as previously described (14, 15). Transposon mutant libraries were selected on peptone-yeast extract rich medium (PYE) supplemented with gentamicin. Depending on the respective library, the plates were incubated at the selection temperatures of 5 °C, 10 °C, 25 °C, or 30 °C. As soon as colonies appeared, the selected mutant libraries were separately pooled off the plates, supplemented with 10% vol/vol dimethyl sulfoxide (DMSO) and stored in a 96-well format at −80 °C for subsequent use.

FRET Microscopy. FRET imaging was performed on a Nikon Eclipse Ti-E inverted microscope with a precisExcite CoolLED light source, a Hamamatsu ORCA-ERA CCD camera, and a Plan Apo λ 100× Oil Ph3 DM objective, combined with a heating unit to maintain an environmental temperature of 25 °C during the imaging. Single time point acquisitions were taken under the acquisition and channel settings according to ref. 12.

CIP Peptide Assay. The CIP peptide was ordered from Thermo Fisher Scientific GENEART. Stocks were kept in 100% DMSO, and the peptide was applied in a final DMSO concentration of 4% to synchronized *Caulobacter* NA1000 wild-type and Δ*pilA* populations prior to FRET microscopy. The swarmer fraction was resuspended in M2 salts, and the CIP peptide was administered to a final concentration of 100 uM.

Data Availability Statement. All data discussed in the paper are available in *SI Appendix*, Tables S1–S9 and Dataset S1.

ACKNOWLEDGMENTS. We thank C. Aquino and R. Schlapbach from the Zurich Functional Genomics Center for sequencing support, and W.-D. Hardt and S. I. Miller for helpful comments on the manuscript. We thank J. Collier and M. Thanbichler for generously providing strains, and S. Loosli and H. Wennemers for help with peptide characterization. This work received institutional support from the Swiss Federal Institute of Technology (ETH) Zürich, ETH Research Grant ETH-08 16-1 to B.C., and Swiss National Science Foundation Grants 31003A_166476, 310030_184664, and CRSII5_177164 to B.C.

1. C. Berne, C. K. Ellison, A. Ducret, Y. V. Brun, Bacterial adhesion at the single-cell level. *Nat. Rev. Microbiol.* **16**, 616–627 (2018).
2. G. Li *et al.*, Surface contact stimulates the just-in-time deployment of bacterial adhesins. *Mol. Microbiol.* **83**, 41–51 (2012).
3. J. Palmer, S. Flint, J. Brooks, Bacterial cell attachment, the beginning of a biofilm. *J. Ind. Microbiol. Biotechnol.* **34**, 577–588 (2007).
4. C. S. Smith, A. Hinz, D. Bodenmiller, D. E. Larson, Y. V. Brun, Identification of genes required for synthesis of the adhesive holdfast in *Caulobacter crescentus*. *J. Bacteriol.* **185**, 1432–1442 (2003).
5. L. Shapiro, Differentiation in the *Caulobacter* cell cycle. *Annu. Rev. Microbiol.* **30**, 377–407 (1976).
6. P. D. Curtis, Y. V. Brun, Getting in the loop: Regulation of development in *Caulobacter crescentus*. *Microbiol. Mol. Biol. Rev.* **74**, 13–41 (2010).
7. H. H. McAdams, L. Shapiro, The architecture and conservation pattern of whole-cell control circuitry. *J. Mol. Biol.* **409**, 28–35 (2011).
8. M. Brilli *et al.*, The diversity and evolution of cell cycle regulation in alpha-proteobacteria: A comparative genomic analysis. *BMC Syst. Biol.* **4**, 52 (2010).
9. C. K. Ellison *et al.*, Obstruction of pilus retraction stimulates bacterial surface sensing. *Science* **358**, 535–538 (2017).
10. I. Hug, S. Deshpande, K. S. Sprecher, T. Pfohl, U. Jenal, Second messenger–mediated tactile response by a bacterial rotary motor. *Science* **358**, 531–534 (2017).
11. C. K. Ellison, D. B. Rusch, Y. V. Brun, Flagellar mutants have reduced pilus synthesis in *Caulobacter crescentus*. *J. Bacteriol.* **201**, e00031-19 (2019).
12. M. Christen *et al.*, Asymmetrical distribution of the second messenger c-di-GMP upon bacterial cell division. *Science* **328**, 1295–1297 (2010).
13. B. Christen *et al.*, High-throughput identification of protein localization dependency networks. *Proc. Natl. Acad. Sci. U.S.A.* **107**, 4681–4686 (2010).
14. B. Christen *et al.*, The essential genome of a bacterium. *Mol. Syst. Biol.* **7**, 528 (2011).
15. M. Christen *et al.*, Quantitative selection analysis of bacteriophage ϕCbK susceptibility in *Caulobacter crescentus*. *J. Mol. Biol.* **428**, 419–430 (2016).

16. B. Zhou *et al.*, The global regulatory architecture of transcription during the *Caulobacter* cell cycle. *PLoS Genet.* **11**, e1004831 (2015).
17. J. M. Schrader *et al.*, Dynamic translation regulation in *Caulobacter* cell cycle control. *Proc. Natl. Acad. Sci. U.S.A.* **113**, E6859–E6867 (2016).
18. M. Kanehisa, M. Furumichi, M. Tanabe, Y. Sato, K. Morishima, KEGG: New perspectives on genomes, pathways, diseases and drugs. *Nucleic Acids Res.* **45**, D353–D361 (2016).
19. S. C. Smith *et al.*, Cell cycle-dependent adaptor complex for ClpXP-mediated proteolysis directly integrates phosphorylation and second messenger signals. *Proc. Natl. Acad. Sci. U.S.A.* **111**, 14229–14234 (2014).
20. A. A. Iniesta, P. T. McGrath, A. Reisenauer, H. H. McAdams, L. Shapiro, A phosphosignaling pathway controls the localization and activity of a protease complex critical for bacterial cell cycle progression. *Proc. Natl. Acad. Sci. U.S.A.* **103**, 10935–10940 (2006).
21. A. Duerig *et al.*, Second messenger-mediated spatiotemporal control of protein degradation regulates bacterial cell cycle progression. *Genes Dev.* **23**, 93–104 (2009).
22. K. K. Joshi, M. Bergé, S. K. Radhakrishnan, P. H. Viollier, P. Chien, An adaptor hierarchy regulates proteolysis during a bacterial cell cycle. *Cell* **163**, 419–431 (2015).
23. R. Wright, C. Stephens, G. Zweiger, L. Shapiro, M. Alley, Caulobacter Lon protease has a critical role in cell-cycle control of DNA methylation. *Genes Dev.* **10**, 1532–1542 (1996).
24. K. Jonas, J. Liu, P. Chien, M. T. Laub, Proteotoxic stress induces a cell-cycle arrest by stimulating Lon to degrade the replication initiator DnaA. *Cell* **154**, 623–636 (2013).
25. K. G. Gora *et al.*, Regulated proteolysis of a transcription factor complex is critical to cell cycle progression in *Caulobacter crescentus*. *Mol. Microbiol.* **87**, 1277–1289 (2013).
26. S. Iyer-Biswas *et al.*, Scaling laws governing stochastic growth and division of single bacterial cells. *Proc. Natl. Acad. Sci. U.S.A.* **111**, 15912–15917 (2014).
27. B. N. Dubey *et al.*, Hybrid histidine kinase activation by cyclic di-GMP–mediated domain liberation. *Proc. Natl. Acad. Sci. U.S.A.* **117**, 1000–1008 (2020).
28. A. Kaczmarczyk *et al.*, Precise timing of transcription by c-di-GMP coordinates cell cycle and morphogenesis in Caulobacter. *Nat. Commun.* **11**, 1–16 (2020).
29. E. Trampari *et al.*, Bacterial rotary export ATPases are allosterically regulated by the nucleotide second messenger cyclic-di-GMP. *J. Biol. Chem.* **290**, 24470–24483 (2015).
30. P. Wassmann *et al.*, Structure of BeF3–modified response regulator PleD: Implications for diguanylate cyclase activation, catalysis, and feedback inhibition. *Structure* **15**, 915–927 (2007).
31. P. H. Viollier, N. Sternheim, L. Shapiro, A dynamically localized histidine kinase controls the asymmetric distribution of polar pili proteins. *EMBO J.* **21**, 4420–4428 (2002).
32. M. Thanbichler, L. Shapiro, MipZ, a spatial regulator coordinating chromosome segregation with cell division in Caulobacter. *Cell* **126**, 147–162 (2006).
33. J. L. Ptacin *et al.*, Bacterial scaffold directs pole-specific centromere segregation. *Proc. Natl. Acad. Sci. U.S.A.* **111**, E2046–E2055 (2014).
34. R. Paul *et al.*, Allosteric regulation of histidine kinases by their cognate response regulator determines cell fate. *Cell* **133**, 452–461 (2008).
35. M. Tomich, D. H. Fine, D. H. Figurski, The TadV protein of *Actinobacillus actinomycetemcomitans* is a novel aspartic acid prepilin peptidase required for maturation of the Flp1 pilin and TadE and TadF pseudopilins. *J. Bacteriol.* **188**, 6899–6914 (2006).
36. C. L. Giltner, Y. Nguyen, L. L. Burrows, Type IV pilin proteins: Versatile molecular modules. *Microbiol. Mol. Biol. Rev.* **76**, 740–772 (2012).
37. J. Mignolet, G. Panis, P. H. Viollier, More than a Tad: Spatiotemporal control of Caulobacter pili. *Curr. Opin. Microbiol.* **42**, 79–86 (2018).
38. L. Craig, K. T. Forest, B. Maier, Type IV pili: Dynamics, biophysics and functional consequences. *Nat. Rev. Microbiol.* **17**, 429–440 (2019).
39. P. Entcheva-Dimitrov, A. M. Spormann, Dynamics and control of biofilms of the oligotrophic bacterium *Caulobacter crescentus*. *J. Bacteriol.* **186**, 8254–8266 (2004).
40. G. Karimova, J. Pidoux, A. Ullmann, D. Ladant, A bacterial two-hybrid system based on a reconstituted signal transduction pathway. *Proc. Natl. Acad. Sci. U.S.A.* **95**, 5752–5756 (1998).
41. A. Waterhouse *et al.*, SWISS-MODEL: Homology modelling of protein structures and complexes. *Nucleic Acids Res.* **46**, W296–W303 (2018).
42. S.-i. Nishiyama *et al.*, Identification of a Vibrio cholerae chemoreceptor that senses taurine and amino acids as attractants. *Sci. Rep.* **6**, 20866 (2016).
43. Z. Zhang, W. A. Hendrickson, Structural characterization of the predominant family of histidine kinase sensor domains. *J. Mol. Biol.* **400**, 335–353 (2010).
44. K. J. Watts, M. S. Johnson, B. L. Taylor, Different conformations of the kinase-on and kinase-off signaling states in the Aer HAMP domain. *J. Bacteriol.* **193**, 4095–4103 (2011).
45. S. P. Wang, P. L. Sharma, P. V. Schoenlein, B. Ely, A histidine protein kinase is involved in polar organelle development in *Caulobacter crescentus*. *Proc. Natl. Acad. Sci. U.S.A.* **90**, 630–634 (1993).
46. C. A. Rodesney *et al.*, Mechanosensing of shear by *Pseudomonas aeruginosa* leads to increased levels of the cyclic-di-GMP signal initiating biofilm development. *Proc. Natl. Acad. Sci. U.S.A.* **114**, 5906–5911 (2017).
47. Y. F. Inclan *et al.*, A scaffold protein connects type IV pili with the Chp chemosensory system to mediate activation of virulence signaling in *Pseudomonas aeruginosa*. *Mol. Microbiol.* **101**, 590–605 (2016).
48. R. A Snyder, C. K. Ellison, G. B. Severin, C. M. Waters, Y. V. Brun, Surface sensing stimulates cellular differentiation in Caulobacter crescentus. https://doi.org/10.1101/844324. (16 November 2019).
49. M. Sangermani, I. Hug, N. Sauter, T. Pfohl, U. Jenal, Tad pili play a dynamic role in Caulobacter crescentus surface colonization. *mBio* **10**, e01237–19 (2019).
50. S. L. Kilmury, L. L. Burrows, Type IV pilins regulate their own expression via direct intramembrane interactions with the sensor kinase PilS. *Proc. Natl. Acad. Sci. U.S.A.* **113**, 6017–6022 (2016).
51. M. Christen *et al.*, DgrA is a member of a new family of cyclic diguanosine monophosphate receptors and controls flagellar motor function in Caulobacter crescentus. *Proc. Natl. Acad. Sci. U.S.A.* **104**, 4112–4117 (2007).
52. U. Römling, M. Gomelsky, M. Y. Galperin, C-di-GMP: The dawning of a novel bacterial signalling system. *Mol. Microbiol.* **57**, 629–639 (2005).
53. L. R. Hoffman *et al.*, Aminoglycoside antibiotics induce bacterial biofilm formation. *Nature* **436**, 1171–1175 (2005).
54. P. A. Cotter, S. Stibitz, C-di-GMP-mediated regulation of virulence and biofilm formation. *Curr. Opin. Microbiol.* **10**, 17–23 (2007).
55. A. J. Merz, C. A. Enns, M. So, Type IV pili of pathogenic Neisseriae elicit cortical plaque formation in epithelial cells. *Mol. Microbiol.* **32**, 1316–1332 (1999).